

Time-dependent self-trapping of Bose-Einstein Condensates in a double-well potential

B. Cui, L. C. Wang, X. X. Yi*
*School of Physics and Optoelectronic Technology,
 Dalian University of Technology, Dalian 116024 China*
 (Dated: September 14, 2018)

Based on the mean-field approximation and the phase space analysis, we discuss the dynamics of Bose-Einstein condensates in a double-well potential. By applying a periodic modulation to the coupling between the condensates, we find the condensates can be trapped in the time-dependent eigenstates of the effective Hamiltonian, we refer to this effect as time-dependent self-trapping of BECs. A comparison of this self-trapping with the adiabatic evolution is made, finding that the adiabatic evolution beyond the traditional(linear) adiabatic condition can be achieved in BECs by manipulating the nonlinearity and the ratio of the level bias to the coupling constant. The fixed points for the system are calculated and discussed.

PACS numbers: 03.65.Bz, 07.60.Ly

I. INTRODUCTION

Bose-Einstein condensates (BECs) in a double-well potential have attracted much attention in the past decades, it provides a useful tool to study fundamental problems in quantum physics at the macroscopic scale and opens the possibility of practical applications, such as high-precision measurements, interferometry and thermometry [1]. Different from Josephson junctions realized in superconductors or superfluids [2, 3], the interatomic interactions in BECs play an important role in its dynamics, leading to many rich and interesting nonlinear effects. Self-trapping [4–7] is one of these interesting phenomena from which much attention has been received in recent years. When the initial population imbalance between the two wells and the nonlinearity in BECs is above a critical value, the amplitude of the Josephson oscillations are extremely compressed and most of the atoms are trapped in one well as theoretically predicted and experimentally observed [7].

The self-trapping is originally defined and studied for a time-independent system (Hamiltonian). Consider a system governed by a time-dependent Hamiltonian, the following questions naturally arise: How can we make the self-trapping happen at a time-dependent state? What are the fixed points in this situation? How do these fixed points behave? We will answer these questions in this paper. In fact, adiabatic dynamics in BECs has been investigated in different regimes, such as Landau-Zener transition [8–16], Rosen-Zener process [17, 18]. Meanwhile, several proposals have been proposed with the stimulated Raman adiabatic passage technique(STIRAP) [19], to coherently manipulate BECs in double-well or triple-well potentials by adiabatically following a spatial dark state of the system [20–24], finding that nonlinearity plays a negative role against adiabatic evolution in some regimes [24]. Different from these works, we discuss here the pos-

sibility of manipulating the BECs to adiabatically follow the instantaneous eigenstate of the system with the help of atom-atom couplings. We find that nonlinearity can help the system to track the instantaneous eigenstates of the system, leading to a self-trapping. By manipulating the nonlinearity and the ratio of the level bias to the coupling constant, adiabatic evolution beyond the traditional adiabatic condition can be achieved in BECs in both symmetric and asymmetric double-well potentials.

The paper is organized as follows. In Sec. II, we introduce the model and transform the equations to the time-dependent representation, choosing the instantaneous eigenstates as the basis. In Sec. III and Sec. IV, we investigate the self-trapping in BECs in a symmetric and an asymmetric double-well potential respectively, and discuss the effect of nonlinearity on the dynamics. Finally, we conclude our results in Sec. V.

II. MODEL

We start with the standard nonlinear two-level model, which describes a BEC in a double-well potential [8, 9, 13]. In a time-independent basis $\{|L\rangle, |R\rangle\}$, the model can be written as [4, 5]

$$\begin{aligned} i\frac{d}{dt}\begin{pmatrix} a \\ b \end{pmatrix} &= \frac{1}{2}\begin{pmatrix} r+ms & v \\ v & -r-ms \end{pmatrix}\begin{pmatrix} a \\ b \end{pmatrix} \\ &\equiv H_0\begin{pmatrix} a \\ b \end{pmatrix}, \end{aligned} \quad (1)$$

where $s = |b|^2 - |a|^2$ stands for the population imbalance between the two wells denoted respectively by $|L\rangle$ and $|R\rangle$. r , v and m characterize the level bias, the tunneling between the two wells and the nonlinearity in BECs, respectively. Here and hereafter, we rescale m , r , v in units of ω , and t in units of $1/\omega$, $\hbar = 1$ has been set, hence all parameters in this paper are of dimensionless. In previous study, the tunneling v is a real parameter, here we discuss a complex tunneling dependent on time through $V = ve^{i\omega t}$, which can be viewed as a nonlinear two-level

*Email:yixx@dlut.edu.cn

system driven by a time-dependent magnetic field [25], $\vec{B} = (B_x, B_y, B_z)$. There are many ways to realize experimentally such a Hamiltonian. For instance, one may simulate this Hamiltonian by a BEC in a double-well potential with the height of the potential barrier modulated and the phases of the two modes mismatched. Define $\cos \beta = \frac{r}{\sqrt{r^2+v^2}}$, $\alpha = 2B_0 = \sqrt{r^2+v^2}$, $\phi = \omega t$, the effective Hamiltonian H_0 (**replace v by $V = ve^{i\omega t}$ and V^* respectively in Eq.(1)**) can be rewritten as,

$$H_0 = B_0(\sin \beta \cos \phi \sigma_x + \sin \beta \sin \phi \sigma_y + \cos \beta \sigma_z) + \frac{1}{2} m s \sigma_z, \quad (2)$$

where B_0 acts as the amplitude of the magnetic field, σ_x , σ_y and σ_z are the Pauli matrices for the two-level system. β behaves as the ratio of the level bias to the coupling constant, α characterizes the amplitude of the driving field, and ϕ represents the swept angle of driving field.

It is easy to write the instantaneous eigenstates of the system, $|E_+\rangle = (\cos \frac{\beta}{2}, \sin \frac{\beta}{2} e^{i\omega t})^T$ and $|E_-\rangle = (-\sin \frac{\beta}{2} e^{-i\omega t}, \cos \frac{\beta}{2})^T$ in the basis $|L\rangle$ and $|R\rangle$, with the corresponding eigenenergy $E_{\pm} = \pm\alpha/2$. After a representation transformation by replacing the original time-independent bases $|L\rangle$ and $|R\rangle$ with the instantaneous energy eigenstates $|E_+\rangle$ and $|E_-\rangle$, we obtain a new set of equation

$$i \frac{d}{dt} \begin{pmatrix} c \\ d \end{pmatrix} = \begin{pmatrix} E_+ + M_1 s + E_{++} & M_2 s + E_{+-} \\ M_2^* s + E_{-+} & E_- - M_1 s + E_{--} \end{pmatrix} \begin{pmatrix} c \\ d \end{pmatrix} \quad (3)$$

with c and d representing the amplitude of the BECs in $|E_+\rangle$ and $|E_-\rangle$, respectively, i.e., $|\psi\rangle = c|E_+\rangle + d|E_-\rangle$. The following notations have been used,

$$s = \cos \beta s_1 + \sin \beta s_2 \\ \equiv \cos \beta (|d|^2 - |c|^2) + \sin \beta (cd^* e^{i\phi} + c^* d e^{-i\phi}),$$

$$\begin{aligned} M_1 &= \frac{m}{2} \cos \beta, \\ M_2 &= -\frac{m}{2} \sin \beta e^{-i\phi}, \\ E_{++} &= -E_{--} \\ &= -i \langle E_+ | \dot{E}_+ \rangle \\ &= \frac{\omega}{2} (1 - \cos \beta), \\ E_{+-} &= E_{-+}^* \\ &= -i \langle E_+ | \dot{E}_- \rangle \\ &= \frac{\omega}{2} \sin \beta e^{-i\phi}. \end{aligned} \quad (4)$$

Here s representing the nonlinearity consists of two types, namely s_1 and s_2 , which correspond to population imbalance and spatial atomic coherence [24], respectively. M_1 and M_2 characterize the strength of nonlinearity in the system. E_{\pm} and $E_{\pm\pm}$ are actually the integrand of the

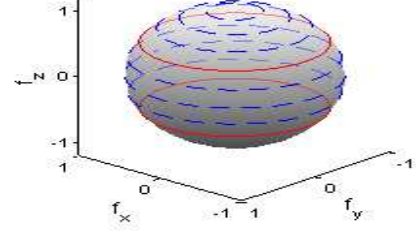


FIG. 1: (color online) Illustration of self-trapping states on the Bloch sphere. The Bloch vectors for these states are $f_x = \sin(2\gamma - \beta) \cos \phi$, $f_y = \sin(2\gamma - \beta) \sin \phi$ and $f_z = \cos(2\gamma - \beta)$. The basis is $\{|L\rangle, |R\rangle\}$. The red-solid lines denote the instantaneous eigenstates of the system and blue-dashed lines represent the other self-trapping states. The parameters chosen are $r = 1$, $v = \sqrt{3}$ and $\beta = \pi/3$.

dynamical phase and Berry phase [26, 27]. E_{+-} and E_{-+} are terms that may induce tunneling between the new bases $|E_+\rangle$ and $|E_-\rangle$, and they are also the parts which lead the adiabatic theorem to break down [28] for the system without nonlinearity. Observing Eq.(3), we find that the nonlinearity may help to track the system on the instantaneous eigenstate of the Hamiltonian, meanwhile the change rate of the Hamiltonian can affect the self-trapping of the BECs on the instantaneous eigenstates, how do they relate to each other?

With the mean-field approximation, the probability amplitudes can be written as $c = |c|e^{i\theta_c}$ and $d = |d|e^{i\theta_d}$. By defining population imbalance and relative phase as $Z = |d|^2 - |c|^2$ and $\Theta = \theta_d - \theta_c$, respectively, we can study the dynamics of the system in its (classical) phase space [4, 10]. However, the situation under study is little bit different, the BECs are driven effectively by a rotating magnetic field with frequency ω , this motivates us to define *pseudo fixed points* by

$$\dot{Z} = 0, \quad \text{and} \quad \dot{\Theta} = \omega, \quad (5)$$

in the phase space, which corresponds to states of the form, $|\psi\rangle = |c||E_+\rangle + |d|e^{i\omega t}|E_-\rangle$ with fixed population difference in the language of wavefunction. We can track this state both in adiabatic and diabatic evolution. For simplicity, we will refer the *pseudo fixed points* as fixed points when no confusion arises. Define $\sin \gamma = |c|$ and $\cos \gamma = |d|$, the state corresponding to the fixed point can be represented in the basis $\{|L\rangle, |R\rangle\}$ as $|\psi\rangle = (\sin(\gamma - \frac{\beta}{2}), \cos(\gamma - \frac{\beta}{2})e^{i\omega t})^T$.

By manipulating γ (location of the fixed points), we can obtain different instantaneous self-trapping states, which maintains the population imbalance and keeps the relative phase matched with the driving field, as shown in Fig. 1. For example, the fixed point $\gamma = 0$ ($Z = 1$) and $\gamma = \frac{\pi}{2}$ ($Z = -1$) represent the instantaneous energy eigenstates $|\psi\rangle = |E_-\rangle$ and $|\psi\rangle = |E_+\rangle$, respectively.

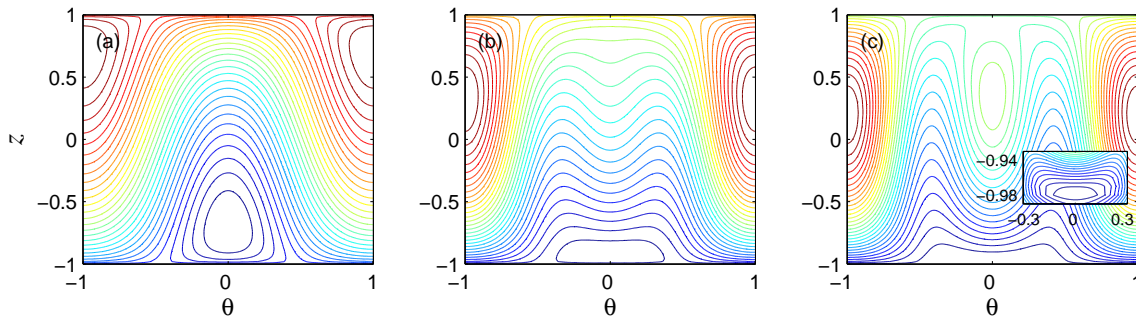


FIG. 2: Phase-space trajectories with different nonlinearity. θ is in units of π . $v = 1$ and $\omega = 1$. The nonlinearity is set as $m = 0$ in (a), $m = 2$ in (b) and $m = 4$ in (c), respectively. For weak nonlinearity, there exist two fixed points. When $|M_2| > |E_{+-}|$ (strong nonlinearity), the other two fixed points appear in the phase-space. The system can be trapped in the pole fixed point (we denote by the pole fixed point the point with Z very close to ± 1 , i.e., near the pole on the Bloch sphere) when nonlinearity is strong enough. The inset in (c) is the enlarged circles around pole fixed point at the bottom of the phase space.

III. SYMMETRIC DOUBLE-WELL POTENTIAL

In this section, we focus on the BECs trapped in a symmetric double-well potential (i.e., $r = 0$, $\beta = \pi/2$) and discuss the self-trapping with different nonlinearity. In this case, the parameters in Eq. (3) reduces to

$$\begin{aligned} s &= s_2, \\ E_{\pm} &= \pm v/2, \\ M_1 &= 0, \\ M_2 &= -\frac{m}{2}e^{-i\phi}, \\ E_{++} &= \omega/2, \\ E_{+-} &= \frac{\omega}{2}e^{-i\phi}, \end{aligned} \quad (6)$$

where only the nonlinearity s_2 from the spatial atomic coherence takes place. In this case, Eq. (3) can be written as

$$i \frac{d}{dt} \begin{pmatrix} c \\ d \end{pmatrix} = \frac{1}{2} \begin{pmatrix} v + \omega & (-ms + \omega)e^{-i\phi} \\ (-ms + \omega)e^{i\phi} & -v - \omega \end{pmatrix} \begin{pmatrix} c \\ d \end{pmatrix}. \quad (7)$$

The system in this limit is interesting because it provides a model to show the nonlinear effect when the nonlinearity appears only in the off-diagonal term. The self-trapping and the adiabatic evolution alike in the sense that both of them can conserve the population on a state. The difference is that the (traditional) self-trapping happens at a time-independent state, while the adiabatic evolution conserves the population on the time-dependent eigenstates of the Hamiltonian. We now show that the self-trapping can appear at a time-dependent state. By the adiabatic theorem, if the system starts in an eigenstate of the Hamiltonian at time $t = 0$, it will evolve to the corresponding eigenstate of the Hamiltonian at later time as long as the Hamiltonian changes slowly enough. For the considered system without nonlinearity ($m = 0$), the adiabatic condition [28] reads

$$A = \omega/2v \ll 1, \quad (8)$$

where A is the adiabatic condition that we will refer to in later discussion. From Eq. (6), we find that the change rate (E_{+-}) of the Hamiltonian affects the number and behavior of fixed points, now we study this effect by the phase space analysis. Define,

$$\begin{aligned} z &= Z = |d|^2 - |c|^2, \\ \theta &= \Theta - \phi = \theta_d - \theta_c - \phi, \end{aligned} \quad (9)$$

where z and θ satisfy

$$\begin{aligned} \dot{z} &= -\omega\sqrt{1-z^2}\sin\theta + \frac{m}{2}(1-z^2)\sin 2\theta, \\ \dot{\theta} &= \frac{\omega z}{\sqrt{1-z^2}}\cos\theta - mz\cos^2\theta + v. \end{aligned} \quad (10)$$

Then we can cast the dynamical system into a classical Hamiltonian

$$H_e(z, \theta) = vz - \frac{m}{2}z^2\cos^2\theta + \frac{m}{4}\cos 2\theta - \omega\sqrt{1-z^2}\cos\theta. \quad (11)$$

By considering $\dot{\theta} = 0$ and $\dot{z} = 0$, we obtain the following equation,

$$z^4 - 2\frac{v}{m}z^3 - \left(1 - \frac{v^2}{m^2} - \frac{\omega^2}{m^2}\right)z^2 + 2\frac{v}{m}z - \frac{v^2}{m^2} = 0. \quad (12)$$

To study the stability of the fixed points, we introduce the Jacobian matrix [29, 30]

$$J = \begin{pmatrix} \partial\dot{z}/\partial z & \partial\dot{z}/\partial\theta \\ \partial\dot{\theta}/\partial z & \partial\dot{\theta}/\partial\theta \end{pmatrix}. \quad (13)$$

It is well known that the eigenvalues of the Jacobian matrix characterize the type of fixed points and determine the stability of them. Two imaginary eigenvalues indicate a stable elliptic fixed point, while two real eigenvalues correspond to an unstable hyperbolic fixed point. So the stable elliptic fixed points can be singled out by calculating eigenvalues of the corresponding Jacobian matrix.

From Eq. (12), we find that the number of the fixed

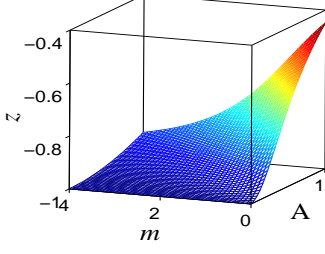


FIG. 3: The pole fixed point versus the nonlinearity m and ω , when v is fixed, ω is proportional to the adiabatic condition A .

points depends on the ratio of the nonlinear parameter M_2 to the adiabatic term E_{+-} . When nonlinearity term is smaller than the adiabatic term, i.e., $|M_2| < |E_{+-}|$, there are only two fixed points, while for strong nonlinearity ($|M_2| > |E_{+-}|$), the other two fixed points appear in the phase space with proper coupling constant v , this was shown in Fig. 2 and in Fig. 4(a). This is interesting, as E_{+-} in linear system can induce population transfer between states $|E_+\rangle$ and $|E_-\rangle$, while it might lead to bifurcation in nonlinear systems. In what follows, we focus on the elliptic fixed point nearest to $z = \pm 1$. This fixed point is stable and describes approximately the instantaneous eigenstate of the system, hence we call it pole fixed point. With strong nonlinearity m , the pole fixed point is very close to $z = \pm 1$, see Fig. 2 and Fig. 3. In this sense we claim that nonlinearity favors the fixed points $z = \pm 1$.

When $A \gg 1$, i.e., the adiabatic condition in linear case has been completely broken down, Eq. (12) can be solved analytically up to the zeroth-order in v/m (we assume that $m \gg v$), there exist three solutions given by

$$z = \begin{cases} \pm \sqrt{1 - \frac{\omega^2}{m^2}} \\ 0 \end{cases}. \quad (14)$$

Eq. (14) tells that we can manipulate the pole fixed point by adjusting the nonlinearity m to satisfy $m \gg \omega$ in this limit, this is numerically confirmed as shown in Fig. 4(c).

IV. ASYMMETRIC DOUBLE-WELL POTENTIAL

In this section, we discuss a more general case that the BECs are trapped in an asymmetric double-well potential ($r \neq 0$). With the same definition for z and θ in Eq. (9), we map the system into a classical phase space. In this

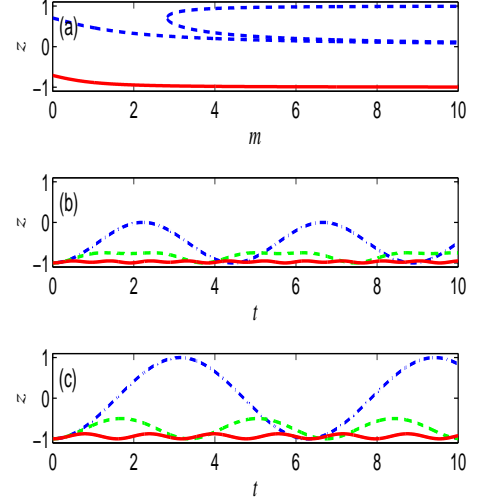


FIG. 4: (color online) (a) The distribution of the fixed points with different nonlinearity. The red-solid line depicts the pole fixed point and blue-dashed lines denote the other fixed points. Parameters chosen are $\omega = 1$ and $v = 1$. (b) Time evolution of the population imbalance with eigenstates of the Hamiltonian as the initial state. Parameters chosen are $\omega = 1$, $v = 1$. $m = 0, 2, 10$ correspond to blue-dash-dotted line, green-dashed line and red-solid line, respectively. (c) is the same as (b), but with different parameters, i.e., $\omega = 1$, $v = 0.01$ and $m = 0, 100, 400$. The system is trapped approximately in one of the instantaneous eigenstates even if adiabatic condition is broken, as the red-solid lines in (b) and (c) show.

case, z and θ satisfy

$$\begin{aligned} \dot{z} &= -\frac{\omega v}{\alpha} \sqrt{1-z^2} \sin \theta \\ &+ \frac{mrv}{\alpha} z \sqrt{1-z^2} \sin \theta + \frac{mv^2}{2\alpha^2} (1-z^2) \sin 2\theta, \\ \dot{\theta} &= \frac{\alpha^2 - \omega r}{\alpha} + \frac{mr^2}{\alpha^2} z + \frac{\omega v}{\alpha} \frac{z}{\sqrt{1-z^2}} \cos \theta \\ &+ \frac{mrv}{\alpha^2} \frac{1-2z^2}{\sqrt{1-z^2}} \cos \theta - \frac{mv^2}{\alpha^2} z \cos^2 \theta. \end{aligned} \quad (15)$$

The effective Hamiltonian and the equation for z can be analytically expressed as

$$\begin{aligned} H_e(z, \theta) &= \frac{m}{2\alpha^2} z^2 (r^2 - v^2 \cos^2 \theta) + \frac{mrv}{\alpha^2} z \sqrt{1-z^2} \cos \theta \\ &- \frac{\omega v}{\alpha} \sqrt{1-z^2} \cos \theta + \frac{\alpha^2 - \omega r}{\alpha} z \\ &+ \frac{mv^2}{4\alpha^2} \cos 2\theta, \end{aligned} \quad (16)$$

$$\begin{aligned} m^2 \alpha^4 z^4 &+ \alpha^4 (\alpha^2 + \omega^2 - m^2 - 2\omega r) z^2 \\ &+ 2m\alpha^3 (r^2 - v^2 - \omega r) z^3 + 2m\alpha (\omega r^3 - \alpha^2 r^2 + \alpha^2 v^2) z \\ &+ m^2 r^2 v^2 - \alpha^2 (\alpha^2 - \omega r)^2 = 0. \end{aligned} \quad (17)$$

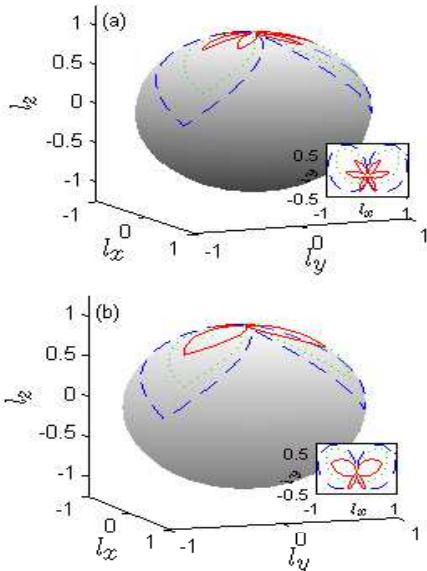


FIG. 5: (color online) (a) Illustration of the biggest-valued fixed points (including stable and unstable ones) with different nonlinearity. (b) The biggest-valued stable elliptic fixed points (pole fixed point) with different nonlinearity. Here $l_x = \sqrt{1-z^2} \cos \beta$, $l_y = \sqrt{1-z^2} \sin \beta$ and $l_z = z$, where z is the population imbalance. Parameters chosen are $\omega = 2$, $\alpha = 1$ and $m = 0, 2, 4$ corresponding to blue-dashed, green-dotted and red-solid lines.

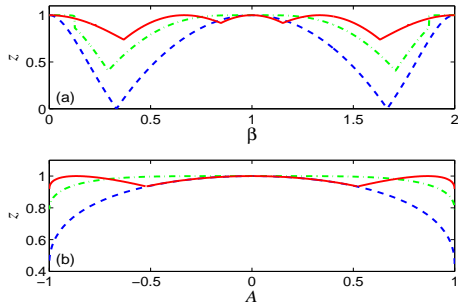


FIG. 6: (color online) The pole fixed point versus β (see (a)) and A (the adiabatic condition parameter, see (b)). β is in units of π . Parameters chosen are $\omega = 2$, $\alpha = 1$. $m = 0, 2, 4$ are for the blue-dashed, green-dash-dotted and red-solid lines respectively.

By the phase space analysis, we find that, different from the symmetric case, the fixed points are determined not only by the nonlinearity m but also by the ratio of the level bias r to the coupling constant v . Without nonlinearity, the adiabatic condition [28] is

$$A = \frac{\omega}{2\alpha} \sin \beta \ll 1. \quad (18)$$

Now we investigate the dynamics of the system under different nonlinearity m and β , which have the same notations as before, while ω and α are fixed corresponding to a constant frequency and amplitude of the driving field. The adiabatic condition becomes $A = \sin \beta \ll 1$, when we set $\omega/2\alpha = 1$. By examining the location of the biggest-valued fixed points with different nonlinearity from adiabatic regime to diabatic regime, we find that the nonlinearity in BEC does play a positive role in the process of adiabatic evolution as shown in Fig. 5 and Fig. 6. When nonlinearity is weak, it pushes the pole fixed point to $z = \pm 1$ at all circumstances, as shown by the green-dotted line in Fig. 5(b). When the nonlinearity becomes strong, bifurcation appears, corresponding to the occurrence of new fixed points in the phase space and the system can evolve on its instantaneous energy eigenstate beyond adiabatic condition at some special β , as shown by the red-solid line in Fig. 6(a). Before closing this section, we would like to address that all fixed points can be easily calculated and analyzed. Aiming to study the self-trapping in the instantaneous eigenstates of the Hamiltonian, we here mainly focus on the fixed point nearest to $z = \pm 1$, discussions on the other fixed points can be carried out in the same way.

Two remarks are now in order. (1) The linear and nonlinear systems discussed here are not independent, the linear system is exactly a limiting case of the nonlinear system with zero nonlinearity. (2) The fixed points are defined based on the basis spanned by the instantaneous eigenstates, so the imbalance of the population represented by z denotes the population difference on the two instantaneous eigenstates, it ranges from -1 to 1 depending on the system parameters. Moreover, the population on the right and left wells can also be manipulated, this can be found via the definition of the instantaneous eigenstates.

V. CONCLUSION

In summary, the time-dependent self-trapping for Bose-Einstein condensates in a double-well potential has been introduced and studied in this paper. Both the atom-atom coupling and the quality which characterize the change of the system play important roles in the self-trapping. Fixed points are calculated and discussed. These results suggest that the nonlinearity can help tracking the instantaneous eigenstates of the time-dependent Hamiltonian, providing a way to manipulate quantum systems.

We are grateful to Dr. Jiangbin Gong for helpful suggestions on early versions of this manuscript. This work is supported by NSF of China under grant Nos. 10775023 and 10935010.

-
- [1] M. R. Andrews, C. G. Townsend, H. J. Miesner, D. S. Durfee, D. M. Kurn, and W. Ketterle, *Science* **275**, 637 (1997); H. J. Wang, X. X. Yi, and X. W. Ba, *Phys. Rev. A* **62**, 023601 (2000); Y. Shin, M. Saba, A. Schirotzek, T. A. Pasquini, A. E. Leanhardt, D. E. Pritchard, and W. Ketterle, *Phys. Rev. Lett.* **92**, 150401 (2004); J. Estève, J. B. Trebbia, T. Schumm, A. Aspect, C. I. Westbrook, and I. Bouchoule, *Phys. Rev. Lett.* **96**, 130403 (2006); G. F. Wang, L. B. Fu, and J. Liu, *Phys. Rev. A* **73**, 013619 (2006); B. V. Hall, S. Whitlock, R. Anderson, P. Hannaford, and A. I. Sidorov, *Phys. Rev. Lett.* **98**, 030402 (2007); U. Hohenester, P. K. Rekdal, A. Borzi, and J. Schmiedmayer, *Phys. Rev. A* **75**, 023602 (2007); J. Esteve, C. Gross, A. Weller, S. Giovanazzi, and M. K. Oberthaler, *Nature (London)* **455**, 1216 (2008).
- [2] S. V. Pereverzev, A. Loshak, S. Backhaus, J. C. Davis, and R. E. Packard, *Nature (London)* **388**, 449 (1997).
- [3] A. K. Sukhatme, Y. Mukharsky, T. Chui, and D. Pearson, *Phys. Rev. Lett.* **411**, 280 (2001).
- [4] A. Smerzi, S. Fantoni, S. Giovanazzi, and S. R. Shenoy, *Phys. Rev. Lett.* **79**, 4950 (1997).
- [5] G. J. Milburn, J. Corney, E. M. Wright, and D. F. Walls, *Phys. Rev. A* **55**, 4318 (1997).
- [6] S. Raghavan, A. Smerzi, S. Fantoni, and S. R. Shenoy, *Phys. Rev. A* **59**, 620 (1999).
- [7] M. Albiez, R. Gati, J. Fölling, S. Hunsmann, M. Cristiani, and M. K. Oberthaler, *Phys. Rev. Lett.* **95**, 010402 (2005).
- [8] B. Wu and Q. Niu, *Phys. Rev. A* **61**, 023402 (2000).
- [9] J. Liu, L. B. Fu, B. Y. Ou, S. G. Chen, D. I. Choi, B. Wu, and Q. Niu, *Phys. Rev. A* **66**, 023404 (2002).
- [10] J. Liu, B. Wu, and Q. Niu, *Phys. Rev. Lett.* **90**, 170404 (2003).
- [11] G. Theocharis, P. G. Kevrekidis, D. J. Frantzeskakis, and P. Schmelcher, *Phys. Rev. E* **74**, 056608 (2006).
- [12] E. M. Graefe, H. J. Korsch, and D. Witthaut, *Phys. Rev. A* **73**, 013617 (2006).
- [13] G. F. Wang, D. F. Ye, L. B. Fu, X. Z. Chen, and J. Liu, *Phys. Rev. A* **74**, 033414 (2006).
- [14] A. P. Itin and S. Watanabe, *Phys. Rev. E* **76**, 026218 (2007).
- [15] A. Altland, V. Gurarie, T. Kriecherbauer, and A. Polkovnikov, *Phys. Rev. A* **79**, 042703 (2009).
- [16] K. Smith-Mannschott, M. Chuchem, M. Hiller, T. Kottos, and D. Cohen, *Phys. Rev. Lett.* **102**, 230401 (2009).
- [17] D. F. Ye, L. B. Fu, and J. Liu, *Phys. Rev. A* **77**, 013402 (2008).
- [18] L. B. Fu, D. F. Ye, C. H. Lee, W. P. Zhang, and J. Liu, *Phys. Rev. A* **80**, 013619 (2009).
- [19] K. Bergmann, H. Theuer, and B.W. Shore, *Rev. Mod. Phys.* **70**, 1003 (1998).
- [20] K. Eckert, M. Lewenstein, R. Corbalán, G. Birkl, W. Ertmer, and J. Mompart, *Phys. Rev. A* **70**, 023606 (2004).
- [21] N. V. Vitanov and B. W. Shore, *Phys. Rev. A* **73**, 053402 (2006).
- [22] M. Rab, J. H. Cole, N. G. Parker, A. D. Greentree, L. C. L. Hollenberg, and A. M. Martin, *Phys. Rev. A* **77**, 061602(R) (2008).
- [23] V. O. Nesterenko, A. N. Nikonov, F. F. de Souza Cruz, and E. L. Lapolli, *Laser Phys.* **19**, 616 (2009).
- [24] C. Ottaviani, V. Ahufinger, R. Corbalan, and J. Mompart, *Phys. Rev. A* **81**, 043621 (2010).
- [25] Qi Zhang, P. Hänggi, and Jianbin Gong, *Phys. Rev. A* **77**, 053607(2008); Jiangbin Gong, Luis Morales-Molina, and Peter Hänggi, *Phys. Rev. Lett.* **103**, 133002 (2009); L. Morales-Molina and J.B. Gong, *Phys. Rev. A* **78**, 041403 (2008).
- [26] B. Simon, *Phys. Rev. Lett.* **51**, 2167 (1983).
- [27] M. V. Berry, *Proc. R. Soc. London A* **392**, 45 (1984).
- [28] M. Born and V. Fock, *Z. Phys.* **51**, 165 (1928).
- [29] S. H. Strogatz, *Nonlinear Dynamics and Chaos* (Addison-Wesley, New York, 1994).
- [30] W. E. Boyce and R. C. Diprima, *Elementary Differential Equations and Boundary Value Problems* (Wiley, New York, 1997).